High Energy Physics and Nuclear Physics

Volume 18, Number 2

Anti-proton-Nucleus Inelastic Scatterings at Intermediate Energies

Li Yangguo

(Department of Physics, Shantou University, Guangdong, China)

The distorted wave of anti-proton is obtained by an optical potential derived from the multiple scattering theory. In the framework of the distorted wave impulse approximation, we discuss the antiproton-nucleus inelastic scattering at intermediate energies. The inelastic differential cross sections of $^{12}C(\bar{p},\bar{p}')^{12}C^*$, 2^+, 3^- states at anti-proton energies from 180 MeV to 1800 MeV are calculated. It is shown that DWIA fitted the experimental data quite well, and theoretical results of inelastic cross sections at higher energies are predicted.

Key words: anti-proton, inelastic scattering, optical potential, distorted wave impulse approximation.

1. INTRODUCTION

More and more attention has been paid to the experimental and theoretical studies of the anti-proton-nucleus elastic and inelastic scatterings recently [1-3]. Since the construction of the high resolution Low Energy Anti-proton Ring (LEAR) at CERN, the anti-proton-nucleon and anti-proton-nucleus scattering experiments at the energies lower than 180 MeV have been successfully performed. Recently, LEAR has been improved and the beam energy of the anti-proton has been increased up to 500 MeV [4] and will possibly reach 1 GeV in the near future. There will be anti-proton-nucleus scattering experiments undertaken at the intermediate energy region (from several-hundred MeV to GeV). Thus, theoretical predictions for $\bar{p}$-A scatterings at the intermediate

Received on July 15, 1992. Supported by the National Natural Science Foundation of China.

energy region are expected. Actually, some theoretical results have already been published [5]. In the frame-work of the multiple scattering theory, by using the basic interaction between anti-proton and nucleus, we derived an anti-proton-nucleus optical potential at the intermediate energy region, and further discussed $\bar{p}$-A elastic scatterings [6]. By employing the optical potential mentioned above and using the distorted wave impulse approximation (DWIA), we study in this paper the anti-proton-nucleus inelastic scattering process. In the following, we would point out that the distorted waves are obtained by using the optical potential derived from the two-body elementary interaction. Meanwhile, the same two-body elementary interaction is used to excite the nucleon in the nucleus. Therefore, in our calculation no new parameters are introduced, but the two-body elementary amplitude which comes from the experimental data [7-9]. This means that there are no free parameters, thus the theoretical uncertainty is avoided. The purpose of this paper is to discuss the characters of the anti-proton inelastic scattering under a strong-absorptive anti-proton optical potential in DWIA at the intermediate energy region. In Section 2, DWIA is briefly summarized, and in Section 3, some calculated results for ^{12}C are given and are compared with the experimental data at 180 MeV. The discussion is made in the final section.

2. OPTICAL POTENTIAL AND DWIA METHOD

According to the multiple scattering theory, we derived the central optical potential as [6]:

$$U^{(\mathrm{Opt})}(r) = V_0 f_V(r) + iW_0 f_W(r), \tag{1}$$

with

$$V_0 = \hbar v_{\bar{N}} \frac{\sigma_{\bar{N}N}}{2} \rho_0 \varepsilon, \tag{1.1}$$

$$W_0 = \hbar v_{\bar{N}} \frac{\sigma_{\bar{N}N}}{2} \rho_0, \tag{1.2}$$

$$f_j(r) = \frac{1}{1 + e^{(r-R_j)/a_j}}, \quad j = V \text{ or } W \tag{1.3}$$

$\sigma_{\bar{N}N}$ is the total $\bar{p}$-N cross section, ε stands for the ratio of the real and imaginary $\bar{p}$-N amplitudes, ρ_0 represents the average nucleon density and $v_{\bar{N}}$ denotes the incident anti-proton velocity. In the DWIA method, one expects solutions of all wanted distorted partial waves of the anti-proton under this optical potential. These solutions satisfy the following equation

$$\left(\frac{d^2}{dr^2} + k^2 - \frac{L(L+1)}{r^2} - \frac{2m_{\bar{p}}(U^{(\mathrm{Opt})}(r) + V_c(r))}{\hbar^2}\right) r\chi_L(kr) = 0, \tag{2}$$

where $V_c(r)$ is the anti-proton-nucleus Coulomb potential. The anti-proton distorted wave function can be expanded as

$$\chi^{(\pm)}(\boldsymbol{k}r) = 4\pi \sum_L i^L Y^*_{LM}(\hat{k}) Y_{LM}(\hat{r}) \chi^{(\pm)}_L(kr), \tag{3}$$

Under DWIA, the T matrix of the anti-proton-nucleus inelastic scattering is

$$\langle \boldsymbol{k}'_{\bar{p}}, f | T | i, \boldsymbol{k}_{\bar{p}} \rangle = \langle \chi^{(-)} \psi_{J_f M_f}(A) | S | \psi_{J_i M_i}(A) \chi^{(+)} \rangle, \tag{4}$$

Table 1
^{12}C optical potential and $\bar{p}N$ two-body amplitude parameters.

$E_{\bar{p}}$ MeV	V_0 MeV	W_0 MeV	r_V fm	r_W fm	$a_V = a_W$ fm	$\sigma_{\bar{p}N}$ (mb)	ε
179.7	−35	−135	1.05	1.2	0.54	149	0.2
294.6	−35	−135	1.05	1.2	0.54	132	0.25
508	−35	−135	1.05	1.2	0.54	110	0.22
1070	−20	−135	1.05	1.2	0.54	92	0.14
1833	−10	−135	1.05	1.2	0.54	81	0.04

with

$$S = \sum_{j=1}^{A} t_{\bar{p}}(j),$$

$t_{\bar{p}}(j)$ is the collision matrix between the anti-proton and the j-th nucleon. $\psi J_i M_i(A)$ and $\psi J_f M_f(A)$ are the initial and final state wave functions of the nucleus, respectively. They are many-body wave functions of an A-nucleon system. By using the technique in the many-body method, we can separate the state of the knocked-out nucleon from the state of the system, and then reduce the T matrix to

$$\langle \boldsymbol{k}'_{\bar{p}}, f | T | i, \boldsymbol{k}_{\bar{p}} \rangle = \langle \boldsymbol{k}'_{\bar{p}} | t_{\bar{p}N} | \boldsymbol{k}_{\bar{p}} \rangle F_{f,i}(\theta), \tag{5}$$

with

$$F_{f,i}(\theta) = \sum_{\substack{Jii' \\ mm'}} B_{Ji} B_{Ji'} I^{ii'}_{mm'}(\theta) C^{J_i M_i}_{jm J_M} C^{J_f M_f}_{j'm' J_M}, \tag{5.1}$$

$$I^{ii'}_{mm'}(\theta) = \int \mathrm{d}^3 r X^{(-)*}(\boldsymbol{k}_{\bar{p}} \cdot \boldsymbol{r}) \varphi^*_{i'm'}(\boldsymbol{r}) \varphi_{im}(\boldsymbol{r}) X^{(+)}(\boldsymbol{k}_{\bar{p}} \cdot \boldsymbol{r}), \tag{5.2}$$

where $\varphi_{jm}(\boldsymbol{r})$ and $\varphi_{j'm'}(\boldsymbol{r})$ are the wave functions of the initial and final states of the excited nucleon during the collision, respectively, $|B_{Jj}|^2$ and $|B_{Jj}|^2$ denote the probabilities of separating $\varphi_{jm}(\boldsymbol{r})$ and $\varphi_{j'm'}(\boldsymbol{r})$ from the many-body wave function, respectively, Θ is the angle between $\boldsymbol{k}_{\bar{p}}$ and $\boldsymbol{k}_{\bar{p}}'$, and $<\boldsymbol{k}_{\bar{p}}'|t_{\bar{p}N}|\ \boldsymbol{k}_{\bar{p}}>$ represents the two-body t matrix in the $\bar{p}$-nucleus, the center of mass system. Associating with the t matrix in the $\bar{p}$-N center of mass system, the DWIA differential cross section of the anti-proton-nucleus inelastic scattering can be expressed as

$$\left(\frac{\mathrm{d}\sigma}{\mathrm{d}\Omega}\right)_{f,i} = \frac{k'_{\bar{p}}}{k_{\bar{p}}} \frac{k_{\bar{p}N}}{k_{\bar{p}N}} \left(\frac{AE'}{E}\right)^2 \left(\frac{\mathrm{d}\sigma}{\mathrm{d}\Omega}\right)_{\bar{p}N \to \bar{p}N} \cdot \overline{\sum_{f,i}} |F_{f,i}(\theta)|^2, \tag{6}$$

where $\left[\frac{\mathrm{d}\sigma}{\mathrm{d}\Omega}\right]_{\bar{p}N \to \bar{p}N}$ is the free anti-proton-nucleon differential cross section, E' represents the total energy of the two-body system, and $k_{\bar{p}}$, $k_{\bar{p}}'$ and $k_{\bar{p}N}$, $k_{\bar{p}N}'$ are the anti-proton incident and outgoing momenta in the $\bar{p}$-nucleus and $\bar{p}$-N systems, respectively. The distorted wave functions in Eq.(3) are solved by using the optical potential. Substituting these wave functions into Eq.(5.2) and performing the angular integration we finally get

$$\overline{\sum_{f,i}} |F_{fi}(\theta)|^2 = \frac{(2I_f+1)}{(2J_i+1)} \sum_{J,\lambda,\nu} \frac{\left| \sum_{j,j'} B_{Jj} B_{Jj'} F^{(\lambda\nu)}(\theta) Q_\lambda \right|^2}{(2\lambda+1)}, \tag{7}$$

with

$$F^{(\lambda\nu)}(\theta) = \sum_{L,L'} i^{L-L'}(4\pi)\hat{L}\hat{\lambda} C^{L0}_{L'-\nu\lambda\nu} C^{L0}_{L'0\lambda0} Y_L^{-\lambda*}(\hat{k}) \cdot I_{LL'}(l'j',lj), \tag{7.1}$$

$$I_{LL'}(l'j',lj) = \int X_{L'}^{(-)*}(k'_{\bar{p}}r)\varphi^*_{l'j'}(r)\varphi_{lj}(r)X_L^{(+)}(k_{\bar{p}}r)r\mathrm{d}r, \tag{7.2}$$

$$Q_\lambda = \frac{1}{\sqrt{4\pi}} \hat{\lambda}\hat{l}\hat{j}\hat{l}'\hat{j}'(-1)^{l+J-\frac{1}{2}-J_i} C^{l'0}_{l0\lambda0} W\left(jlj'l';\frac{1}{2}\lambda\right) W(J_ijJ_fj';J\lambda), \tag{7.3}$$

where $\hat{j} \equiv \sqrt{2j+1}$, L and L' specify the angular momenta of the incoming and outgoing the distorted partial waves, respectively. If the anti-proton-nucleon elementary process, namely the two-body scattering amplitude is obtained, the optical potential of the anti-proton distorted waves can be determined. After solving the partial wave function $X_L^{(\pm)}(k_{\bar{p}}r)$ with the optical potential the energy level structure wave function $\varphi_{jl}(r)$ of the nucleon in nucleus, $F^{(\lambda\nu)}(\Theta)$ is entirely determined, and then the differential cross section of the inelastic scattering can be obtained. In summary, the inelastic process is determined by the two-body interaction and the nucleon states which induce the inelastic transition.

3. CALCULATED DIFFERENTIAL CROSS SECTION OF INELASTIC SCATTERING FOR ^{12}C NUCLEUS

Since there exist the experimental differential cross sections of the anti-proton-^{12}C inelastic scattering for ^{12}C excited states (2^+, 4.4 MeV) and (3^-, 9.6 MeV) at the incident energy of anti-proton $E_{\bar{p}}$ = 179.7 MeV, we study the DWIA anti-proton-^{12}C inelastic scattering, and hope that by theoretically fitting experimental data at 179.7 MeV, the differential cross section at higher energies can be predicted. The anti-proton-nucleon scattering amplitude can be expressed as

$$f_{\bar{p}N}(q) = \frac{ik\sigma_{\bar{p}N}(1-i\varepsilon)}{4\pi} \cdot e^{-\frac{1}{2}\beta^2 q^2}, \tag{8}$$

The experimental values of $\sigma_{\bar{N}N}$, ε and β at several energies are listed in Table 1. The strength of the optical potential in Eqs.(1), (1.1) and (1.2) are determined. The parameters of the potential are also listed in Table 2. Because this optical potential can fit the experimental elastic differential cross section data of $\bar{p}$-^{12}C at $E_{\bar{p}}$ = 179.7 MeV [6], it is believed that at higher energies, the elastic differential cross section can also be described by the same optical potential. Moreover, using this optical potential to derive the distorted wave function in DWIA is self-consistent. The two-body amplitude (namely, the two-body differential cross section) in Eq.(6) is taken as the result in Eq.(8). Since only the inelastic scattering differential cross section at the forward semisphere or even at the small angular region is considered, the forward amplitude can approximately be used to estimate $\left[\frac{\mathrm{d}\sigma}{\mathrm{d}\Omega}\right]_{\bar{p}N\to\bar{p}N}$.

For the low energy level structure of ^{12}C, in the DWIA frame, we consider those configurations whose ground states can be excited via single collision. ^{12}C is a closed shell nucleus, one can consider the closed $1p_{3/2}$ shell as the ground state. The main configurations of the 2^+(4.4 MeV) and 3^-(9.6 MeV) states are $(p^{-1}_{3/2}\, p_{1/2})$ and $(p^{-1}_{3/2}d_{5/2})$, respectively. Instead of choosing the harmonic oscillator wave function, the wave function $\varphi_{jm}(r)$ in Eq.(7.2) is chosen by solving the bound state wave function

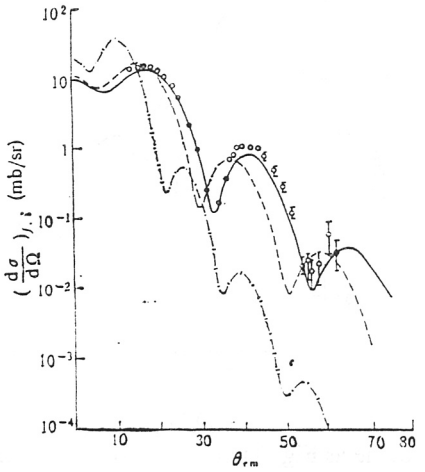

Fig. 1

Theoretical inelastic differential cross section of $^{12}C(\bar{p},\bar{p}')^{12}C^*$ (2^+,4.4 MeV) where the solid curve denotes $E_{\bar{p}}$ = 179.7 MeV, the dashed curve represents $E_{\bar{p}}$ = 232 MeV, the dashed-dotted curve stand for $E_{\bar{p}}$ = 565 MeV, and the points are the experimental data at $E_{\bar{p}}$ = 179.7 MeV.

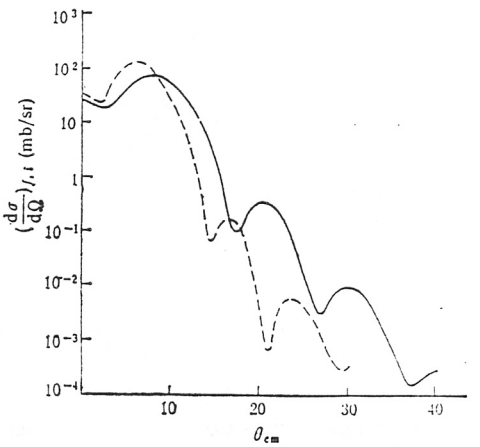

Fig. 2

Same as Fig. 1 where the solid curve denotes $E_{\bar{p}}$ = 1070 MeV, and the dashed curve represents $E_{\bar{p}}$ = 1833 MeV.

of nucleon with the some *nlj* values under the mean potential. This mean potential is in the Saxon-Woods type, with the radius of ^{12}C to be R = 2.93 fm, the diffuseness parameter to be a = 0.677 fm and the depth of the mean potential to be $V_0 \approx$ 50-65 MeV, which is determined by the binding energies of the states. The binding energies of the ground state and 2^+ and 3^- states are 10.64 MeV, 6.2 MeV and 1 MeV, respectively. Thus, there are no free parameters in choosing nucleon wave functions in Eq.(7.2).

The differential cross section of $^{12}C(\bar{p},\bar{p}')^{12}C^*$ at $E_{\bar{p}}$ = 179.7 MeV is calculated first. The excited states of ^{12}C are 2^+(4.4 MeV) and 3^-(9.6 MeV). The results are plotted in Figs. 1 and 3 in solid curves. The experimental values are shown in figures too. From these figures, it is shown that the theoretical results in DWIA can well describe the anti-proton-nucleus inelastic scattering. The calculated results at higher anti-proton energies are given in Figs. 1-4. In order to compare with the results in [5], we take $E_{\bar{p}}$ = 232, 565, 1070 and 1833 MeV in Figs. 1-2.

The calculation is performed by using the modified DWUCK4 [10] program. The partial wave functions $X_L^{(\pm)}$ is solved in terms of the optical potential. The bound states wave function $\varphi_{ij}(r)$ is solved under the Saxon-Woods potential and then the transition density $\rho_{f,i}(r)$ is obtained, and $I_{LL'}(l'j',lj)$ is calculated. The partial wave value L is taken as high as 80 when the energy reaches to 1 GeV. Finally, $F^{(\lambda\nu)}(\Theta)$ is exactly calculated in DWIA.

4. DISCUSSION

The optical potential is obtained by using the impulse approximation via the multiple scattering, while the p-nucleus inelastic scattering calculation is completed via a single inelastic collision and DWIA. It means that the incident anti-proton collides with the nucleons in nucleus several times, one of which is an inelastic transition. The characters of the $\bar{p}$-A inelastic scattering are entirely determined

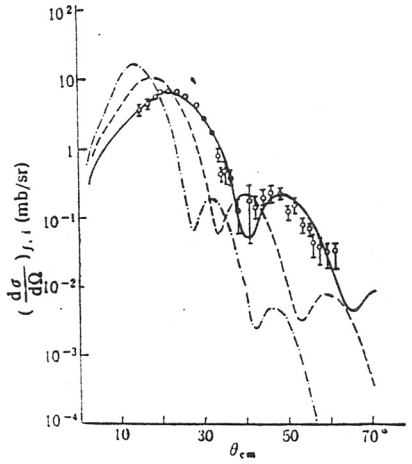

Fig. 3

Theoretical inelastic differential cross section of $^{12}C(\bar{p},\bar{p}')^{12}C^*$ (3^-, 9.6 MeV) where the solid curve denotes $E_{\bar{p}}$ = 179.7 MeV, the dashed curve represents $E_{\bar{p}}$ = 294.8 MeV, the dashed-dotted curve stand for $E_{\bar{p}}$ = 508 MeV, and the points are the experimental data at $E_{\bar{p}}$ = 179.7 MeV.

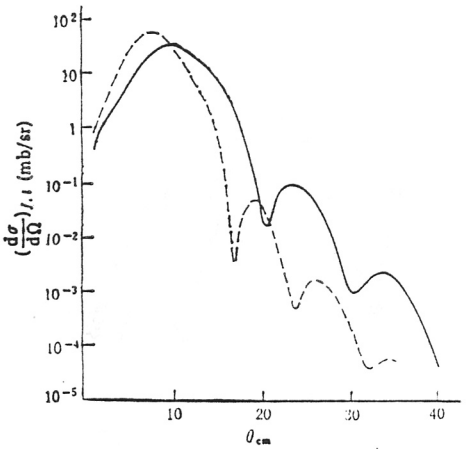

Fig. 4

Same as Fig. 3 where the solid curve denotes $E_{\bar{p}}$ = 1070 MeV, the dashed curve stands for $E_{\bar{p}}$ = 1833 MeV.

by the two-body collision t matrix and the transition density between corresponding nucleon states, $\rho_{f,i}(r) = \varphi^*_{l'j'}(r)\varphi_{lj}(r)$. There are no free parameters except the experimental data of the two-body collision. In comparison with the low energy inelastic scattering discussed with the phenomenal anti-proton-nucleus optical potential earlier [3], although this investigation is also in the DWIA frame, the distorted wave obtained by using the optical potential is more microscopic. The good agreement between the calculated result and the experimental data at $E_{\bar{p}}$ = 179.7 MeV shows that our calculation at higher energies is reliable.

In this calculation, the nucleon wave function $\varphi_{lj}(r)$ is solved in the mean potential well. The transition form factor $\rho_{f,i}(r)$ obtained by using this wave function is more reliable than that calculated in terms of the harmonic oscillator wave function. The former $\rho_{f,i}(r)$ is much stronger than the later one at the region outside the nucleus. Due to the strong absorption, the distorted wave of the anti-proton mainly appears outside the nucleus surface [3]. Therefore, $I_{L,L'}(l'j',lj)$ mainly comes from the contribution outsider the nucleus. That is why the strength and diffraction pattern in this calculation and [3] are quite different, and why by using the exact wave function, one can fit the experimental data at $E_{\bar{p}}$ = 179.7 MeV so well. We believe that our results at higher energies are reliable, and can be referred in the future experiment.

The incident anti-proton energies chose for the 2^+ state inelastic scattering in Figs. 1 and 2 are the same as those in [5], where the Glauber multiple scattering theory was used. Comparing our DWIA results with those in [5], we find some evident differences. Although the diffraction patterns are similar at the same anti-proton incident energy, the positions of the peaks and dips in [5] were located at the smaller angles than those in this calculation. As the incident energy of the anti-proton increases this deviation becomes larger. At the high energy region, say higher than 1 GeV, the differential cross section given in [5] decreased with the increasing angle so fast that the differential cross section became very small beyond 20°. But our results at 20°-30° are in the order of 10^{-3} mb/sr and are detectable. In [6], we pointed out the difference between the optical model and Glauber theory in the

elastic scattering calculation. Here, we also find the difference between the DWIA method and Glauber theory in the inelastic scattering calculation. This is a notable phenomenon. We hope that these results will be checked by the further theoretical investigations and new experiments.

REFERENCES

[1] D. Garreta *et al.*, *Phys. Lett.*, **B135**(1984), p. 266; **B139**(1984), p. 464; **B149**(1984), p. 64; **B151**(1985), p. 473.
[2] S. Janouin *et al.*, *Nucl. Phys.*, **A451**(1986), p. 541.
[3] Li Yangguo, *High Energy Phys. and Nucl. Phys.* (Chinese Edition), **13**(1989), p. 433.
[4] A. Martin *et al.*, *Nucl. Phys.*, **A487**(1988), p. 567.
[5] W. H. Ma *et al.*, *Phys. Rev.*, **C44**(1991), p. 615.
[6] Li Yangguo, *High Energy Phys. and Nucl. Phys.*, **17**(1993), p. 199.
[7] R. Klapisch *et al.*, *Nucl. Phys.*, **A434**(1985), p. 222.
[8] P. Jenni *et al.*, *Nucl. Phys.*, **B94**(1975), p. 1.
[9] H. Kaseno *et al.*, *Phys. Lett.*, **B61**(1976), p. 203; **B68**(1977), p. 481.
[10] P. D. Kunz, DWUCK4 Program.